International Research Journal of Engineering and Technology (IRJET) e-ISSN: 2395 -0056
Volume: 03 Issue: 12 | Dec -2016 www.irjet.net p-ISSN: 2395-0072

Synthesis and Magnetic Properties Investigations of Hematite-Activated Carbon with TiO_2 -Anatase Nanoparticles Composite for Application of Wastewater Treatment at Belbis Drainage-Egypt

Yasser A.M. Abdulhady*

Water Treatment and Desalination Unit, Desert Research Center, Cairo, Egypt
****Corresponding author - Tel: +2 01016941598; fax: +2 0226389069***

E-mail address: Yasser_vip6@hotmail.com & yousefyaser_2002@yahoo.com

---

ABSTRACT

In this study, magnetic iron oxide nanoparticles (Gamma-Fe_2O_3) composite with activated carbon and TiO_2 with a size range of 10-50 nm were prepared by the modified controlled chemical co-precipitation method from the solution of ferrous/ferric salts, activated carbon powder and titanium isopropoxide solution in alkaline medium. In the process isopropanol was used as surfactant to prevent agglomeration. The prepared nanoparticles were characterized by X-ray diffraction (XRD) analysis, scanning electron microscopy (SEM) and vibrating-sample magnetometer (VSM) and FT-IR. XRD indicated the sole existence of inverse cubic spinel phase of magnetic iron oxide nanoparticles (Gamma-Fe_2O_3). VSM patterns indicated low magnetic properties of nanocomposite due to the effect of activated carbon. The removal efficiency of iron, copper and manganese from wastewater of Belbis by the new prepared iron oxide nanocomposite after treatment were observed to be 91.42 %, 90.81 % and 92.96 %, respectively in synthesized solution. Reduction percent of nitrate and phosphate from wastewater were 86.20 % and 95.86 %, respectively. The new prepared iron oxide nanocomposite had new physical and chemical characterization by new additives methodology that had high removal efficiency of heavy metals, nitrates and phosphates upon 90-100 % of inorganic pollutants. This research concerned with copper and manganese removal from wastewater using magnetic nanoparticles (MNPs) coated by titanium oxide and activated carbon. New methodology experiment results showed that 0.05g/100ml sonicated for 25 minutes at pH 7 and 35^{0}C.

Keywords: Magnetic iron oxide nanoparticles (Gamma-Fe_2O_3), nanocomposite, nano-activated carbon, magnetic iron oxide coated TiO_2, modified co-precipitation method, wastewater treatment.

1. INTRODUCTION

Metal oxide nanoparticles have wide applications, including their use as a semiconductor or thermoelectric material, but they are also used in biomedical applications as drug delivery systems for treatment applications.[1,2] The traditional methods for obtaining metal oxide nanoparticles are based on chemical and physical modification a negative effect on the environment.[1] The production of metal oxide nanoparticles has received increasing attention recently because it is a novel process for the development of treatment.[3] Co-precipitation method is a standard way to synthesize MNPs (metal oxides and iron) from aqueous salt solutions. This is done by the addition of a base at room temperatures or variable temperature. Iron oxide nanoparticles (either Fe_3O_4 or γ-Fe_2O_3) are usually synthesized in an aqueous medium which chemical reaction may be written as:

$$M^{2+} + 2Fe^{3+} + 8OH^- \rightarrow MFe_2O_4 + 4H_2O$$

Where M can be Fe^{2+}, Mn^{2+}, Co^{2+}, Cu^{2+}, Mg^{2+}, Zn^{2+} and Ni^{2+}. Complete precipitation should be expected at a pH levels between 8 and 14, with a stoichiometric ratio of 2:1 (Fe^{3+}/M^{2+}) in a non oxidizing oxygen environment.[4] Magnetite nanoparticles (Fe_3O_4) are not very stable under ambient conditions, and are easily oxidized to be a maghemite or dissolved in an acidic medium. Therefore, magnetite particles can be subjected to deliberate oxidation to convert them into a maghemite.[5] The size, shape, and composition of the MNPs depends to large extent on the type of salts used (*e.g.* chlorides, sulfates, nitrates), the M^{2+}/Fe^{3+} ratio, the reaction temperature, the pH value, type of base, the mixing rate, ionic strength of the media, the addition sequence and bubbling of nitrogen gas are all important. Another most important factor influencing the synthesis is the iron

concentration which generally the optimum values are between 39 and 78 mM. In the synthesis of Fe_3O_4, precipitation at temperatures below 60 °C typically produces an amorphous hydrated oxy hydroxide that can be easily converted to Fe_2O_3, while higher reaction temperatures (>80 °C) favor the formation of Fe_3O_4.[6,7] The suitable pH for the rapid formation of Fe_3O_4 is attained by the addition of excess amounts of the base. The product showed a brownish color, an indication of the presence of Fe_2O_3, if the precipitation temperature was below 60 °C or insufficient NH_4OH was added.[8] Hong *et al.* [9] observed that when Fe_3O_4 nanoparticles precipitated using NH_4OH instead of NaOH a better crystalline, higher saturation magnetization and smaller size can be observed.[10] The sol-gel process is a suitable wet route to the synthesis of nano-structured metal oxides.[11,12] This process is based on the hydroxylation and condensation process, originating a "sol" of nano-metric particles. From the review showed that the property of a gel depends on the structure reacted during the sol stage of the sol-gel process. The major parameters that affect on the kinetics, growth reactions, hydrolysis, condensation reactions, structure and properties of the gel formed are solvent, temperature, concentration of the metal salt, pH, and agitation.[13,14,15] For example, it has been reported that γ-Fe_2O_3 nanoparticles in a size range between 6 and 15 nm can be obtained after a direct heat treatment of the gels at a temperature of 400 °C.[16] Nanotechnology contains the study and use of materials at nanoscale dimensions (nano-material sizes of ≤100 nm), which have the different physiochemical properties exhibited by nano-materials from the same materials at a larger scale. The large surface area and highly active surface sites of nanoparticles have ability a wide range of applications magnetic iron oxide nanoparticles that have multiple practical applications, such as physics, medicine, and biology.[17,18,19]

2. EXPERIMENTAL and MATERIALS

Ferric chloride hexahydrate ($FeCl_3.6H_2O$), ferrous chloride tetra-hydrate ($FeCl_2.4H_2O$) and ammonium hydroxide (NH_4OH) purchased from Merck. All acids used were of the highest purity available were obtained from Merck**.** Activated carbon purchased from Sigma-Aldrich and TiO_2 was obtained from Titanium (IV) isopropoxide (TTIP) was dissolved in absolute ethanol and distilled water was added to the solution.

2.1. Preparation of the activated carbon with TiO_2-Anatase coated iron oxide nanoparticles

The magnetic nanoparticles (MNPs) were prepared, according to Hong et al., 2006; Indira, and Lakshmi, 2010. Briefly, $FeCl_2.4H_2O$ and $FeCl_3.6H_2O$ (molar ratio of Fe^{3+}/Fe^{2+}=2/1) were mixed with corresponding volume of TTIP then added isopropanol in beaker with vigorous stirring at 500 rpm at 80 ^oC. Co- Precipitation occurs with the addition of ammonium hydroxide (NH_4OH) as precipitating agent to the solution. The color of solution changed from black to whitish black and finally grays as dominant color then, after calcinations at 400^oC changed to green color. The precipitate obtained was washed twice with deionized water and three times with ethanol.

2.2. Sample Instrumentation

The XRD pattern of activated carbon with TiO_2 coated MNPs was obtained using a X-ray diffractometer Schimadzu model: A PAN analytical X-rays diffraction equipment model Expert PRO with secondary mono-chromator, Cu-radiation (λ=1.54A^0) at 50k.v.,40 M.A and scanning speed 0.02^o /sec. Magnetic properties of the particles were assessed with a vibrating-sample magnetometer (VSM, Homade 2tesla). A magnet (Φ 17.5×20 mm, 5500 O e) was utilized for the collection of magnetic particles**.** Basing on the results of measurements, coercivity, remanence and saturation of samples have been determined, from each powder sample a certain amount of sample has been portioned out, put into another container and weighted. The VSM measurements have been performed on every sample. FT-IR spectra were measured in a transmission mode on a spectrophotometer (PerkinElmer Spectrum Version 10.03.09) Spectrum Two Detector $LiTaO_3$ was used for separating the solid and liquid during the preparation samples. The samples were pressed pellets of a mixture of the powder with KBr. The micrographs of prepared particles were obtained using a Scanning Electron Microscope using SEM Model Quanta 250 FEG (Field Emission Gun).

2.3. Examine nano-composite efficiency

Batch adsorption studies were performed by mixing MNPs with 50 ml of the synthesized wastewater in a flask. For pH adjustment we used standard 0.1M HCl and 0.1M NaOH solutions. Put the solution mixture of MNPs with wastewater solution in sonicator for different time. After adsorption reached equilibrium, the adsorbent was conveniently separated via an external magnetic field and the solution was collected for metal concentration measurements. MNPs were washed thoroughly with deionized water to neutrality. The concentrations of metal ions were measured by a plasma-atomic emission spectrometer

(ICP-AMS, Optima 3000XL, PerkinElmer) in accordance with the Standard Method. In order to obtain reproducible experimental results, the adsorption experiments were carried out at least 3 times.

3. RESULTS and DISCUSSION

3.1. Mechanism of Hematite -Activated Carbon with TiO_2 -Anatase Nanoparticles Composite.

Hydroxylation of the ferrous and ferric ions formed at pH > 8-10 by the precipitation with addition of NH_4OH with drop wise of NaOH. The inorganic salt of ferric ion reacts with NH_4OH and forms FeOOH, which, upon heating, further produce into Fe^{2+} and OH^- ions, which consequently assists in the development of Fe_2O_3 ions according to the chemical reactions. The iron oxide nanoparticles formed in solution with addition of titanium isopropoxide solution with a definite concentration and activated carbon. The nanocomposite mixture has larger surface area than individual nanoparticles. These advantages increase the reduction percent of removal heavy metals. The addition of TiO_2 in reaction to form nano-composite coated the iron oxide nanoparticles. This composite had more specific functional group and more free electrons in dispersion solution that can increase the reduction percent of removal heavy metals.

3.2. Characterization of the nano-composite

3.2.1. Infrared Spectroscopy (FT-IR)

Figure (1) Absorption peaks at 510 cm−1and 540 cm−1 indicated to the Fe–O vibration related to the hematite and two absorption peaks at 2,924 and 2,854 cm−1 were attributed to the asymmetric CH_2 stretching and the symmetric CH_2 stretching, respectively.[20] The bands due to C–O stretching mode were merged in the very broad envelope centered on 1250 cm−1 arising from C–O, C–O–C stretches and C–O–H bends vibrations of iron oxide nanoparticles. The aliphatic C–H stretching, in 1320 and 1390 cm−1 were due to C–H bending vibrations. The broad band at 530-660 cm−1 is likely due to the vibration of the Ti–O bonds in the TiO_2 lattice.[21] The broad peak in 460 cm^{-1} related to iron oxide NPs banding with TiO_2. The IR band at 3455 cm^{-1} can be assigned to the stretching modes of surface H_2O molecules or to an envelope of hydrogen-bonded surface OH groups.

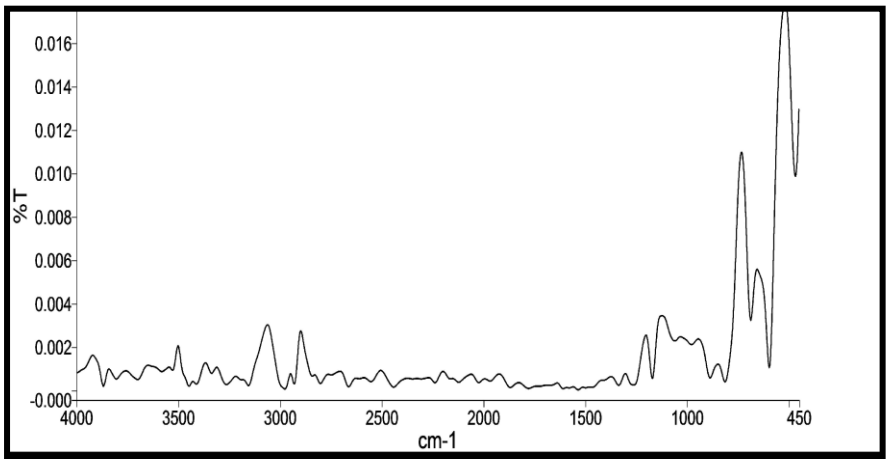

Figure – 1: FT-IR spectra of hematite nanoparticles composite with activated carbon and TiO_2

3.2.2. X-Ray Diffraction Analysis (XRD)

Figure (2) showed peaks at $2\theta = 25^0, 27^0, 33.5^0, 35.5^0, 44.5^0, 49.5^0, 54.5^0$ corresponding to the diffractions of crystal faces, TiO_2 anatase, hematite, active carbon and magnetite spinal structure. The positions and relative intensities of the reflection peak of Fe_3O_4 and Fe_2O_3 MNPs agree with the XRD diffraction peaks of standard Fe_2O_3 samples.[22] Sharp peaks showed that Fe_3O_4 and Fe_2O_3 nanoparticles have well crystallized structure.

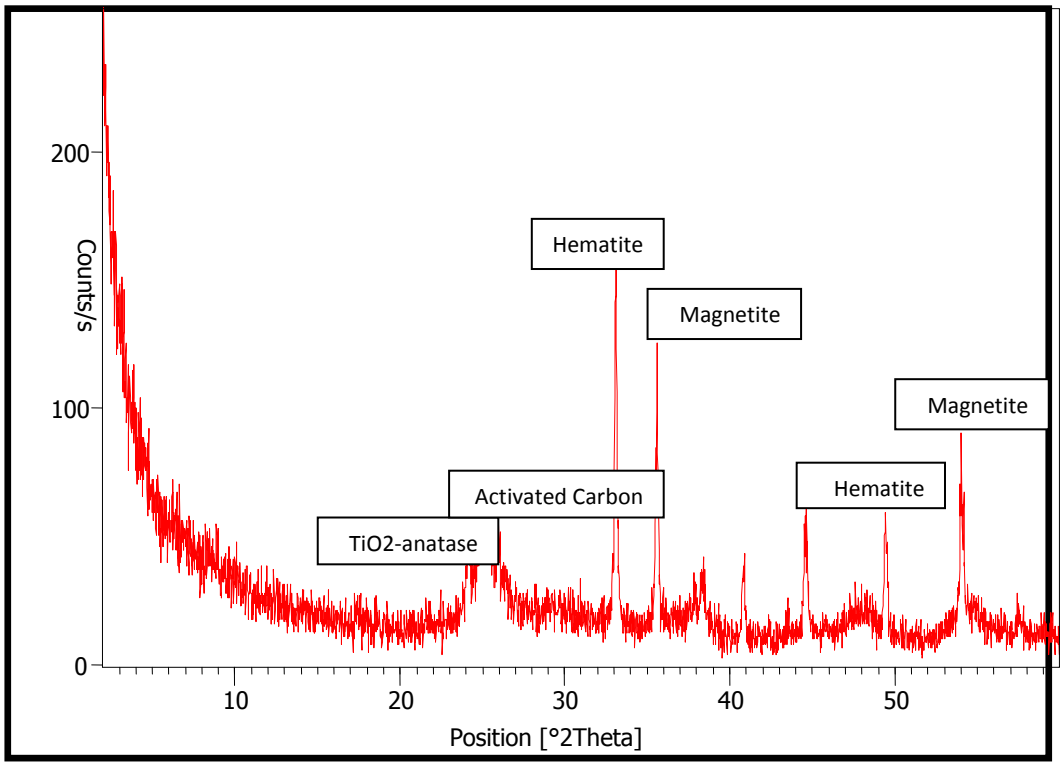

Mineral Name	Chemical Formula	Semi-Quant [%]
Hematite	$Fe_2 O_3$	**25**
Titanium oxide	TiO_2	**15**
Magnetite	$Fe_3 O_4$	**30**
Activated carbon	**AC**	**30**

Figure – 2: XRD pattern of hematite nanoparticles composite with activated carbon and TiO_2

3.2.3. Scanning Electron Micrograph (SEM)

SEM images in Fig (3) showed the surface of nano- composite of hematite nanoparticles with activated carbon and, which confirms that the cubic and spherical shape of hematite nanoparticles merged with TiO_2 and activated carbon in bending structure. The SEM photo showed the homogenous surface and distribution with smoothly surface and homogenous pores and size.

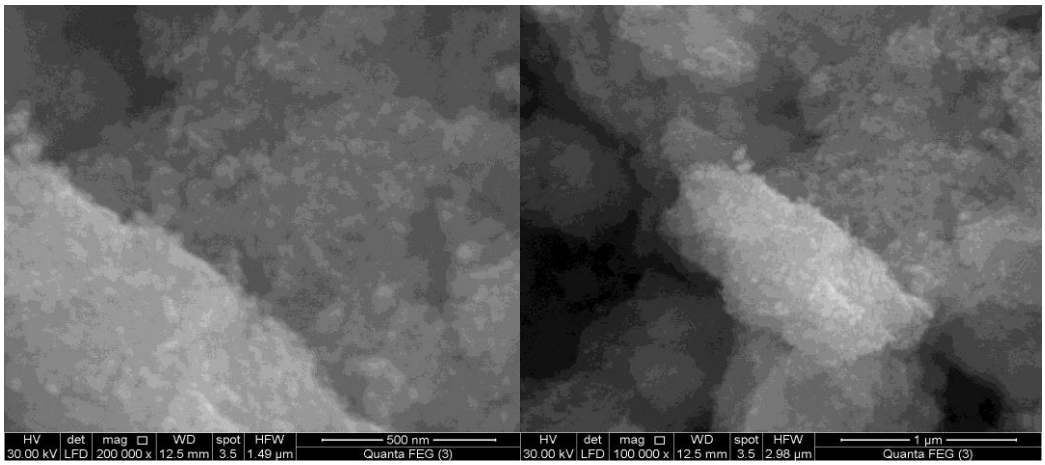

Figure – 3: Scanning Microscope (SEM) for iron oxide nanocomposite with TiO_2/Activated carbon

3.2.4. Particle size analysis of iron oxide nanocomposite with TiO_2/Activated carbon

As shown in fig (4) .The nanoparticles intensity weighting was 75.6 nm, volume weighting was 35.4 nm and number weighting was 16.4 nm.
Fig. (4) Show that the mean diameter of nanocomposite material ranges around 42.4 nm. This reading means that the obtained results of reduction percent of prepared nano iron composite depends mainly on the size and shape with availability of dispersion percent in solution.

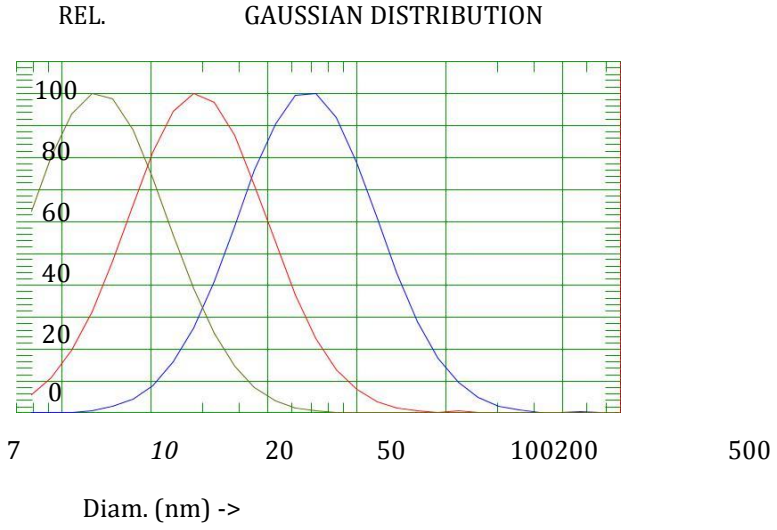

Figure – 4: Particle size distribution of iron oxide nanocomposite with TiO_2/Activated carbon

3.3. Effect of iron oxide nanocomposite with TiO_2/Activated carbon on wastewater treatment

3.3.1. Removal of iron, copper and manganese metals by iron magnetic nanocomposite.

Table (1) showed that the raise level of iron, copper and manganese metals were in permissible standard level. Before treatment the concentration of iron in wastewater was 5.83 ppm as shown in table (1) and it decreased to 0.56 ppm as shown in table (2) after treatment with **iron oxide nanocomposite with TiO_2/Activated carbon**. This inhibition indicated that the adsorption efficiency of prepared nanocomposite was (91.42 %) as shown in table (3) and the nano-composite had a nanosized

shape with large surface area at optimal condition done. Concentration of copper after treatment decreased to 2.40 ppm from 24.82 ppm before treatment as shown in table (2) with reduction percent 90.33 %. The concentration of manganese in wastewater before treatment by nano-composite was 9.17 ppm and after treatment reached to 1.59 ppm with reduction percent 92.96 % table (3)

3.3.2. Removal of nitrate and phosphates by iron oxide nanocomposite with TiO_2/Activated carbon

Table (4) showed that the ability of magnetic nanocomposite **iron oxide nanocomposite with TiO_2/Activated carbon** for removal of nitrate group and phosphate derivatives. The adsorption efficiency (mean reduction percent) of adsorbed nitrate on nanocomposite particles was 86.20 %. The reaction mechanism of adsorption depends on the formation of weak interaction between hydroxyl group and lone pair of electrons on nitrogen atom.

3.3.3. Removal of phosphate content by magnetic iron oxide nanocomposite with TiO_2/Activated carbon

In table (4), the reduction percent of phosphate group adsorbed on nanocomposite particles the mean reduction percent was 95.86 %. The increase of reduction percent caused by the increasing of adsorption and desorption of phosphate group on nanocomposite particles and largest molecular weight of phosphate group.

Table – 1: Analysis of heavy metals in ppm before treatment

Parameter	Permissible limit	A (Cu)	B (Fe)	C (Mn)
	----	8.21 PH	5.84 PH	7.01 PH
Aluminum, mg/l	<0.2	0.950	2.010	0.020
Boron, mg/l	<0.5	0.489	0.290	1.175
Cadmium, mg/l	<0.005	0.002	0.001	0.001
Cobalt, mg/l	<0.05	0.019	0.003	0.001
Chromium, mg/l	<0.05	0.020	0.020	0.020
Copper, mg/l	<0. 5	24.82	0.013	0.009
Iron, mg/l	<0.5	0.470	5.83	0.030
Manganese, mg/l	<0.3	0.005	0.140	9.17
Molybdenum, mg/l	<0.01	0.030	0.001	0.003
Nickel, mg/l	<0.1	0.933	0.006	0.002
Lead, mg/l	<0.05	0.010	0.050	0.017
Vanadium, mg/l	<0.01	0.010	0.010	0.010
Zinc, mg/l	**<5**	**0.950**	**1.010**	**0.002**

Table – 2: Analysis of heavy metals in ppm after treatment

Parameter	Permissible limit	A (Cu)	B (Fe)	C (Mn)
	----	8.21 PH	5.84 PH	**7.01 PH**
Aluminum, mg/l	<0.2	0.350	0.560	0.020
Boron, mg/l	<0.5	0.489	0.290	0.750
Cadmium, mg/l	<0.005	0.002	0.001	0.001
Cobalt, mg/l	<0.05	0.019	0.003	0.001
Chromium, mg/l	<0.05	0.020	0.020	0.020
Copper, mg/l	<0. 5	2.40	0.003	0.001
Iron, mg/l	<0.3	0.170	0.56	0.010
Manganese, mg/l	<0.5	0.005	0.040	1.59
Molybdenum, mg/l	<0.01	0.010	0.001	0.003
Nickel, mg/l	<0.1	0.20	0.006	0.002
Lead, mg/l	<0.05	0.010	0.050	0.017
Vanadium, mg/l	<0.01	0.010	0.010	0.010
Zinc, mg/l	**<5**	**0.950**	**1.010**	**0.002**

Table – 3: Reduction percent of copper & Iron and manganese before and after treatment by iron oxide nanocomposite with TiO_2/Activated carbon of Contaminated waters

Serial	Copper/ ppm			Iron/ ppm			Manganese/ ppm		
	B.T	A.T	R %	B.T	A.T	R %	B.T	A.T	R %
A	24.82	2.40	90.33	0.47	0.17	63.82	0.00	0.00	0.00
B	0.013	0.003	76.92	5.85	0.56	90.42	0.14	0.01	92.85
C	0.009	0.001	88.88	0.03	0.01	66.66	9.173	1.59	82.66
S. S	32.89	3.02	90.81	64.58	5.54	91.42	49.32	3.47	92.96

S.S: Synthesized solution; B.T: Before treatment; A.T: After treatment; R: Reduction%

Table – 4: Reduction percent of nitrate and phosphate by Nanocomposite before and after treatment of polluted water

Serial	NO3-N ppm P.L: 10 to 50 mg/l			PO4-P ppm P.L: 10 to 30 mg/l		
	B.T	A.T	R %	B.T	A.T	R %
A	75.74	10.45	86.20	65.35	2.70	**95.86**
B	95.10	15.36	83.84	52.07	4.90	**90.58**
C	124.25	42.41	65.86	75.63	5.30	**92.99**
S.S	40.56	5.65	86.07	60.29	4.96	**91.77**

S.S: Synthesized solution; B.T: Before treatment; A.T: After treatment; R: Reduction%; P.L: permissible limit

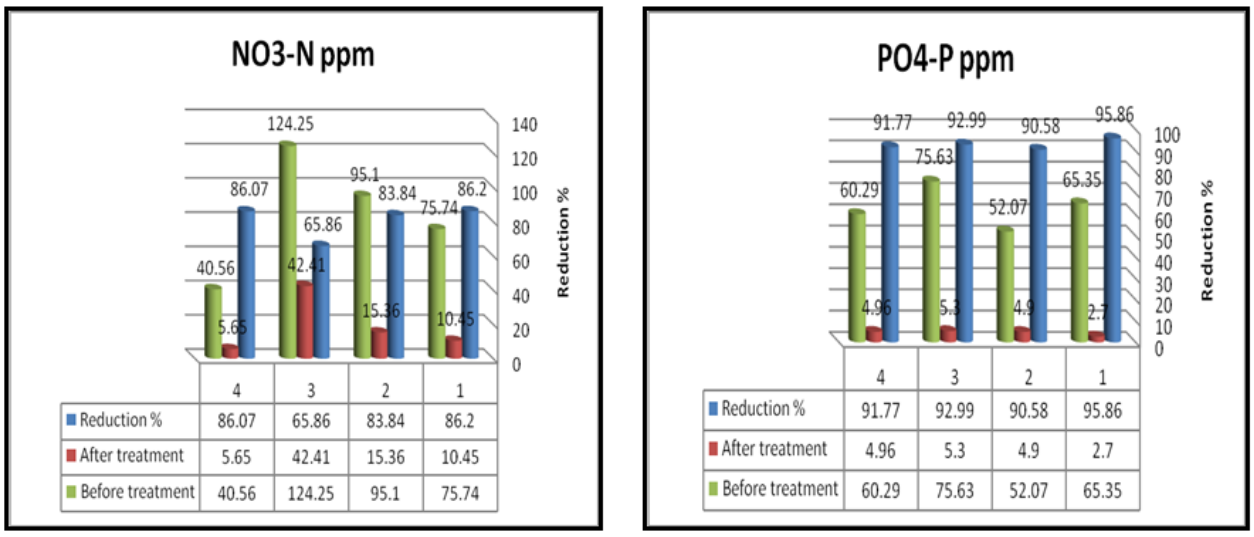

Figure – 5: Reduction percent of nitrate and phosphate by Nanocomposite before and after treatment of polluted water

Table 5. Effect of different conditions with iron concentration

N. Conc. g/100L	Iron		
	B.T	A.T	R %
30	64.58	20.33	68.51
50	64.58	15.61	75.82
100	64.58	10.74	83.36
200	64.58	12.54	80.58

Time Min.	Iron		
	B.T	A.T	R %
5	64.58	15.50	75.99
10	64.58	8.78	86.40
15	64.58	8.80	86.37
20	64.58	8.91	86.20

PH	Iron		
	B.T	A.T	R %
5	64.58	26.54	58.90
6	64.58	13.65	78.86
7	64.58	11.50	82.19
8	64.58	16.71	74.12

R. Temp. °C	Iron		
	B.T	A.T	R %
20	64.58	20.43	68.36
25	64.58	11.22	82.62
30	64.58	16.87	73.87
35	64.58	27.98	56.67

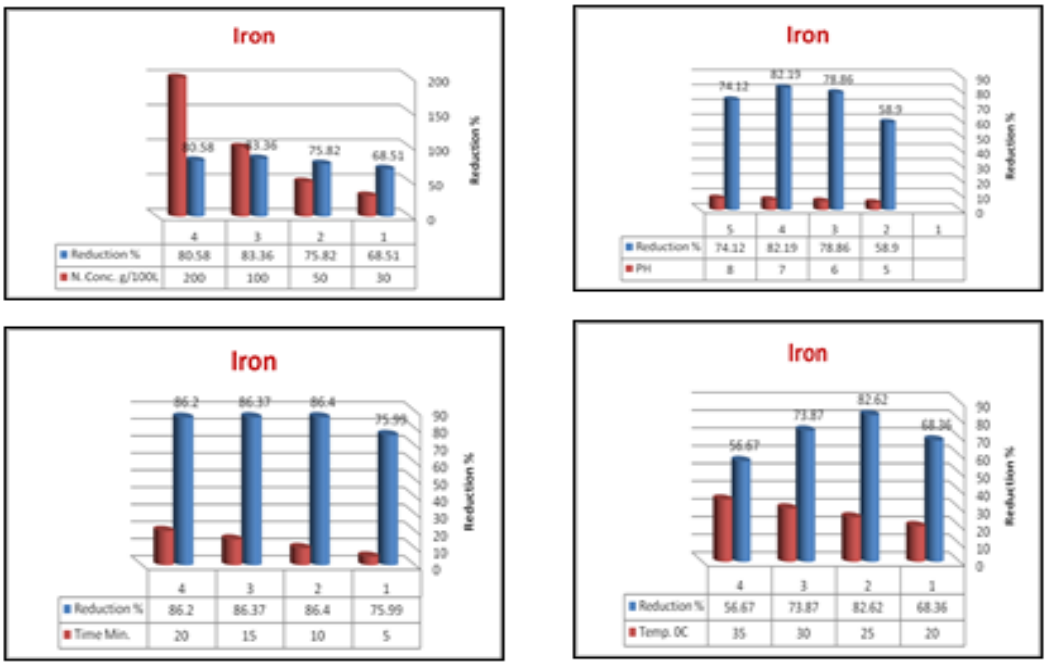

Figure – 6: Effect of different conditions with iron concentration

Table – 6: Effect of different conditions with copper concentration

N. Conc. g/100L	Copper		
	B.T		R %
30	32.89	0.015	83.39
50	32.89	0.025	86.86
100	32.89	0.05	91.21
200	32.89	0.10	88.17

R. Time Min.	Copper		
	B.T	A.T	R %
5	32.89	10.73	67.37
15	32.89	7.92	75.91
25	32.89	1.46	95.56
40	32.89	3.50	89.35

PH	Copper		
	B.T	A.T	R %
5	32.89	9.67	70.59
6	32.89	4.65	85.86
7	32.89	1.82	94.46
8	32.89	6.21	81.11

Temp.^{0}C	Copper		
	B.T	A.T	R %
20	32.89	8.76	73.36
25	32.89	1.21	96.32
30	32.89	1.86	94.34
35	32.89	5.54	83.15

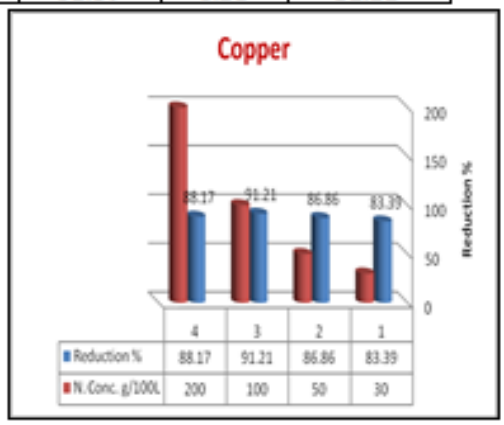

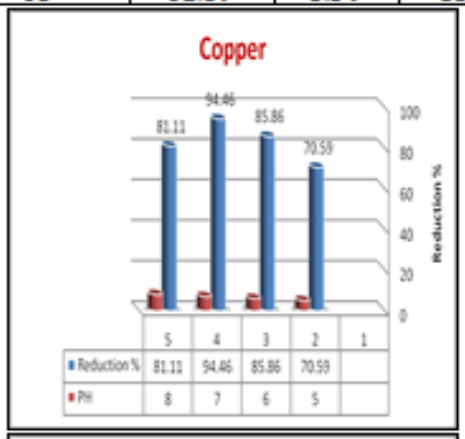

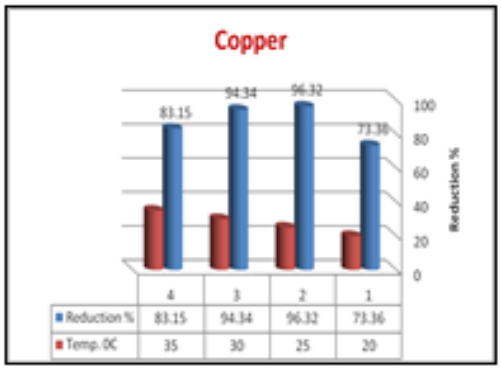

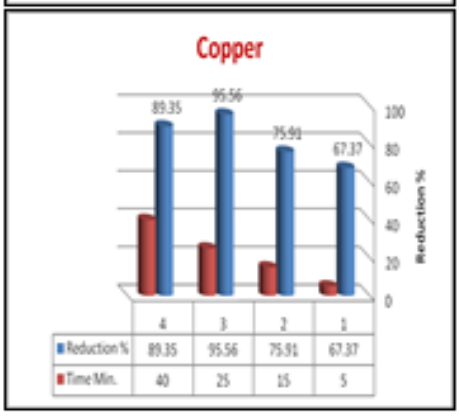

Figure – 7: Effect of different conditions with copper concentration

Table – 7: Effect of different conditions with manganese concentration

N. Conc. g/100L	Manganese		
	B.T	A.T	R %
30	49.32	9.74	80.25
50	49.32	5.06	89.74
100	49.32	1.58	96.79
200	49.32	2.49	94.95

R. Time Min.	Manganese		
	B.T	A.T	R %
5	49.32	10.71	**78.28**
15	49.32	3.66	**92.57**
25	49.32	1.12	**97.72**
40	49.32	2.18	**95.57**

PH	Manganese		
	B.T	A.T	R %
5	49.32	10.26	**79.19**
6	49.32	4.91	**90.04**
7	49.32	1.07	**97.83**
8	49.32	2.98	**93.95**

R. Temp. °C	Manganese		
	B.T	A.T	R %
20	49.32	4.21	**91.46**
25	49.32	1.65	**96.65**
30	49.32	1.97	**96.00**
35	49.32	3.80	**92.29**

B.T: Before treatment; A.T: After treatment; R: Reduction%

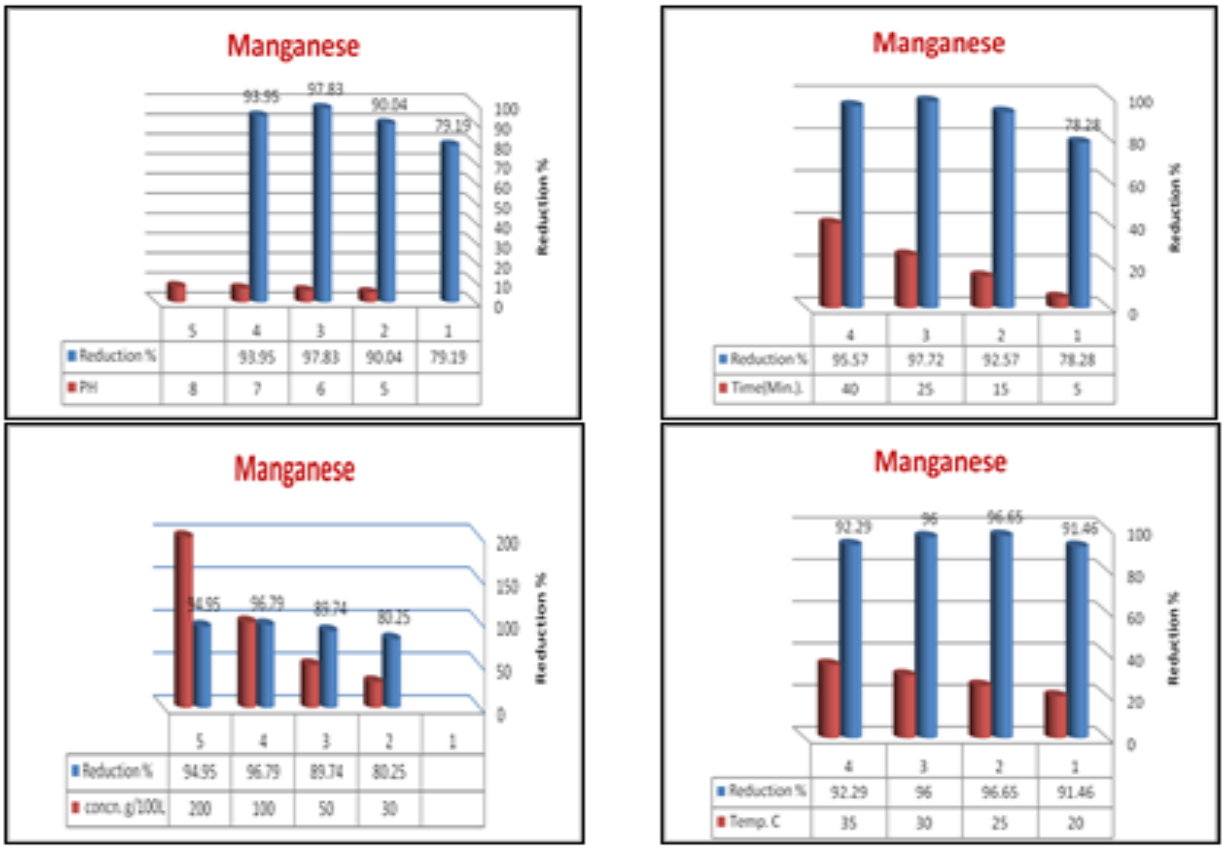

Figure – 8: Effect of different conditions with manganese concentration

4. CONCLUSION

Removal of heavy (toxic) metals was the main goal of this paper. Magnetic Hematite -Activated Carbon with TiO_2 -Anatase Nanoparticles have an effective reduction percent. The removal efficiency of iron, copper and manganese from wastewater of Belbis by the new prepared iron oxide nanocomposite after treatment were observed to be 91.42 %, 90.81% and 92.96 %, respectively in synthesized solution. Reduction percent of nitrate and phosphate from wastewater were 86.20 % and 95.86 %, respectively. The characterization analysis by different instruments showed that iron oxide coated by TiO_2 and active carbon was in the nano-sized range. Active carbon enhanced the nano particles more dispersion efficiency. The adsorption process is a function of pH, reaction time, adsorbent concentration and temperature.

5. FUTURE IMAGE RESEARCH

It is recommended to design a prototype to apply this technique in industry. Target future research will be Synthesis of new nano-composite of iron oxide with natural low economic to produce high yield of reduction percent.

Reference

1. N. Chomchoey, D Bhongsuwan. and T. Bhongsuwan, "Magnetic Properties of Magnetite Nanoparticles Synthesized by Oxidative Alkaline Hydrolysis of Iron Powder," Kasetsart J. (Nat. Sci.), 44, 2010, pp. 963 - 971.

2. L. T. M. Hoa, T. T. Dung, T. M. Danh, N. H. Duc and D. M. Chien, "Preparation of Drug Nanoparticles by an Emulsion Evaporation Method," J Phys Conf Ser (JPCS), vol. 187, no. 1, 2009, 012048.

3. H.Y.C. Acar, R.S. Garaas, F. Syud, P. Bonitatebus and A. M. Kulkarni, "Superparamagnetic Nanoparticles Stabilized by Polymerized PEGylated Coatings," J. Magn. Magn. Mater., vol. 293, no. 1, 2005, pp. 1–7.

4. H. Jung, J.W. Kim, H. Choi, J.-H. Lee and H.-G. Hur, "Synthesis of Nanosized Biogenic Magnetite and Comparison of its Catalytic Activity in Ozonation," Appl. Catal. B , vol. 83, 2008, pp. 208–213.

5. P. Kanhed, S. Birla, S. Gaikwad, A. Gade, A.B. Seabra, O. Rubilar, N. Duran and M. Rai, "*In Vitro* Antifungal Efficacy of Copper Nanoparticles Against Selected Crop Phatogenic Fungi," Mater. Lett., vol. 115, 2014, pp.13–17.

6. M. Vukovic, Z. Brankovic, D. Poleti, A. Recnik and G. Brankovic, "Novel Simple Methods for the Synthesis of Single-phase Valentinite Sb_2O_3," J. Sol-Gel Sci. Technol., vol. 72, 2014, pp. 527–533.

7. A.K. Jha, K. Prasad and K. Prasad, "A Green Low-cost Biosynthesis of Sb_2O_3 nanoparticles. *Biochem. Eng. J.* **2009**, *43*, 303–306.

8. A.K. Jha, K. Prasad and K. Prasad, "Biosynthesis of Sb_2O_3 Nanoparticles: A Low-cost Green Approach," Biotechnol. J., vol. 4, 2009, 1582–1585.

9. R. Y. Hong, S. Z. Zhang, Y. P. Han, H. Z. Li, J. Ding, and Y. Zheng, "Preparation, Characterization and Application of Bilayer Surfactant-stabilized Ferrofluids," Powder Technology, vol. 170, 2006, pp. 1-11.

10. A.B. Seabra, and N. Duran, "Nitric Oxide-releasing Vehicles for Biomedical Applications," J. Mat. Chem., vol. 20, 2010, 1664–1637.

11. Y. Cui and C.M. Liber, "Functional Nanoscale Electronic Devices Assembled Using Silicon Nanowire Building Blocks," Science, vol. 291, 2001, pp. 851-853.

12. T. Qiu, X.L. Wu, Y.F. Mei, G.J. Wan, P.K. Chu and G.G. Siu, "From Si Nanotubes to Nanowires: Synthesis, Characterization, and Self-assembly," J. Cryst. Growth, vol. 277, no. 1-4, 2005, pp. 143-148.

13. L.L. Hench," Bioceramics: From Concept to Clinic," J. Am. Ceram. Soc. , vol. 74, no. 7, 1991, pp. 1487-1510.

14. W. Suchanek and M. Yoshimura, "Processing and Properties of Hydroxyapatite-based Biomaterials for Use as Hard Tissue Replacement Implants," J. Mater. Res., vol. 13, no. 1, 1998, pp. 94-117.

15. K.S. Ten-Huisen, R.I. Martin, M. Klimkiewicz and P.W. Brown, "Formation and Properties of a Synthetic Bone Composite: Hydroxyl Apatite-collagen," J. Biomed. Mater. Res., vol. 29, no. 7, 1995, pp. 803-810.

16. W.L. Suchanek, P. Shuk, K. Byrappa, R.E. Riman, K.S. Ten Huisen, and V.F. Janas, "Mechanochemical-hydrothermal Synthesis of Carbonated Apatite Powders at Room Temperature," Biomaterials, vol. 23, 2003, pp. 699-710.

17. S.A. Corr, "Metal Oxide Nanoparticles," Nanoscience, vol. 1, 2013, pp. 180–234.

18. P.S. Haddad and A.B. Seabra, "Biomedical Applications of Magnetic Nanoparticles. In Iron Oxides: Structure, Properties and Applications, Martinez, A.I., Ed.; Nova Science Publishers, Inc.: New York, NY, USA, vol. 1, 2012, pp. 165–188.

19. N. Durán, and A.B. Seabra, "Metallic Oxide Nanoparticles: State of the Art in Biogenic Syntheses and their Mechanisms," Appl. Microbiol. Biotechnol., vol. 95, 2012, pp. 275–288.

20. Y.F. Shen, J. Tang, Z.H. Nie, Y.D. Wang, Y. Ren and L. Zuo, "Preparation and Application of Magnetic Fe3O4 Nanoparticles for Wastewater Purification," Sep. Purif. Technol., vol. 68, 2009,pp. 312–319.

21. Y. Gao, Y. Masuda, Z. Peng, T. Yonezawa, K. Koumoto, "Room Temperature Deposition of a TiO2 Thin Film from Aqueous Peroxotitanate Solution," J. Mater. Chem., vol. 13, no. 3, 2003, pp. 608-613.

22. M. Mahdavi, M.B. Ahmad, M.J. Haron, Y. Gharayebi, K. Shameli and B. Nadi, "Fabrication and Characterization of SiO2/(3-Aminopropyl) Triethoxysilane-coated Magnetite Nanoparticles for Lead(II) Removal from Aqueous Solution," J. Inorg. Organomet. Polym., vol. 23, 2007, pp. 599–607.